JASMAC Conference of the Japan Society of Microgravity Appllication

OS2-3

ISS-ELF で計測した La_2O_3–Nb_2O_5 二元系融液の物性とガラス形成能との相関

Correlation between the glass forming ability and physical properties of the La_2O_3–Nb_2O_5 binary melts measured using the ISS–ELF

増野敦信 [1,*], 小山千尋 [2], 小原真司 [3], 佐々木俊太 [4], 渡邊勇基 [2], 水野章敏 [5], 手跡雄太 [1], 渡邉学 [1], 石川毅彦 [2]

Atsunobu MASUNO[1,*], Chihiro KOYAMA[2], Shinji KOHARA[3], Shunta SASAKI[4], Yuki WATANABE[2], Akitoshi MIZUNO[5], Yuta SHUSEKI[1], Manabu WATANABE[1], and Takehiko ISHIKAWA[2]

[1] 京都大学，Kyoto University
[2] 宇宙航空研究開発機構，Japan Aerospace Exploration Agency
[3] 物質・材料研究機構，National Institute for Materials Science
[4] 東北大学，Tohoku University
[5] 函館工業高等専門学校，National Institute of Technology, Hakodate College
* Correspondence: masuno.atsunobu.3k@kyoto-u.ac.jp

Abstract: The La_2O_3–Nb_2O_5 binary system binary system represents a unique example of glass formation via levitation processing, despite lacking conventional network-forming oxides. This system exhibits two distinct glass-forming regions at La_2O_3-rich and Nb_2O_5-rich compositions, setting it apart from typical oxide glasses. To investigate its glass-forming ability, the temperature dependence of density, viscosity, and surface tension was measured over a wide temperature range using the electrostatic levitation furnace aboard the International Space Station (ISS–ELF). The melt density exhibited a linear decrease with increasing temperature. Viscosity measurements above the melting point revealed that both La_2O_3-rich and Nb_2O_5-rich melts are fragile yet glass-forming, with a fragility index (m) of approximately 80. Moreover, the activation energy derived from the temperature dependence of viscosity was higher for glass-forming compositions than for those prone to crystallization. These results suggest that activation energy is a useful indicator for evaluating glass-forming ability across a broad compositional range, including both glass-forming and non-glass-forming regions. The ISS–ELF experiments thus offer valuable insights into glass formation in unconventional oxide systems.

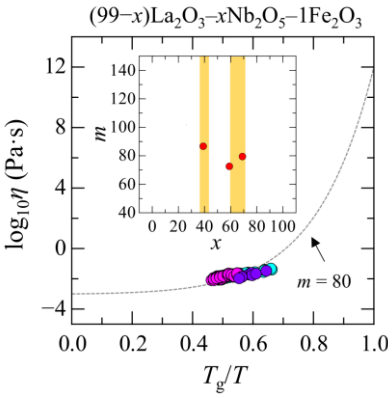

Keywords: Oxide glass, Density, Viscosity, Surface tension

1. Introduction

Over the past two decades, levitation techniques have enabled the formation of glasses without conventional network-forming (NWF) oxides such as SiO_2 and B_2O_3. Binary glasses based on Al_2O_3-, TiO_2-, Nb_2O_5-, WO_3-, MoO_3-, Ga_2O_3-, and Ta_2O_5 have been successfully produced using the methods. These glasses often exhibit exceptional physical properties, including high refractive indices with low wavelength

dispersion, high elastic moduli, and pronounced magneto-optical effects[1]. These superior properties are attributed to their densely packed glass structures, which lack the traditional tetrahedral network connectivity found in conventional oxide glasses[2]. Despite these advances, the mechanisms underlying glass formation in the absence of three-dimensional networks remain poorly understood. Since glass forms through the cooling of a melt, it is essential to obtain thermophysical data such as temperature-dependent density, viscosity, and surface tension over a wide temperature range, from above the melting point to the supercooled region. The electrostatic levitation furnace (ELF) is particularly well suited for these measurements because it maintains the levitated melt in an almost perfectly spherical shape, allowing for high-accuracy evaluation[3]. On Earth, levitation of oxide melts is technically challenging due to the high electric fields required to counteract gravity. These conditions usually necessitate a high-vacuum environment, which also promotes significant evaporation of volatile melt components. In contrast, the ELF installed on the Japanese Experiment Module "Kibo" aboard the International Space Station (ISS) enables measurements under near-atmospheric pressure, minimizing evaporation and enabling stable levitation of oxide melts[4].

In this study, we focus on the La_2O_3–Nb_2O_5 binary system. Previous experiments using an aerodynamic levitation furnace demonstrated that some compositions in this system can form colorless, transparent glasses with exceptionally high refractive indices and low wavelength dispersion, even in the absence of network formers[5]. Notably, the glass-forming region is divided into two separate domains: one rich in La_2O_3 and the other rich in Nb_2O_5. Between these two domains lies a compositional range where vitrification does not occur. Thermal properties, including the glass transition temperature, vary significantly between these regions. Structural analyses have shown clear differences in the connectivity of the glass network depending on the composition[6]. These results suggest that the thermophysical properties of the melts are key to understanding the differences in glass-forming ability and the non-vitrifying nature of specific compositions. Therefore, this study aims to investigate the thermophysical behavior of La_2O_3–Nb_2O_5 melts across a wide composition range to elucidate the fundamental factors that govern glass formation in this system[7].

2. Experimental

High-purity powders of La_2O_3, Nb_2O_5, and Fe_2O_3 were mixed in stoichiometric proportions to prepare samples with the composition $(99-x)La_2O_3$–xNb_2O_5–$1Fe_2O_3$ (x = 29, 39, 49, 59, 69, 79, 89, and 99). Fe_2O_3 was added to enhance absorption of the 980 nm semiconductor laser used in the ISS–ELF experiments. The mixed powders were melted using an aerodynamic levitation (ADL) furnace to form spherical ceramic precursors. Three spherical samples were prepared for each composition, weighed, and placed into designated sample holders, which were then delivered to the International Space Station (ISS) aboard the H-II Transfer Vehicle 7 (HTV7). All subsequent measurements were remotely operated from the Tsukuba Space Center of JAXA.

The ELF chamber was filled with dry air, nitrogen, or argon at a pressure of 2 atm. Each sample was ejected from the holder into the chamber using a rod and then levitated by an electrostatic field. Stabilization at the chamber center was achieved using three pairs of orthogonally arranged electrodes, with voltage fine-tuning to ensure precise positioning. Heating was performed by four 980 nm diode lasers (40 W each) arranged tetrahedrally for uniform irradiation. Feedback control was employed to maintain levitation stability. Upon melting, the oxide samples assumed nearly perfect spherical shapes due to surface tension under microgravity conditions. Magnified images of the samples were acquired using ultraviolet backlighting at each temperature. Temperatures were measured using a pyrometer operating in the wavelength range of 1.45–1.8 μm. The density ρ of the melts was calculated using the formula $\rho = m_s/V$, where m_s is the mass of the sample and V is its volume. The volume V was determined from image analysis of the levitated sphere. The surface tension γ and viscosity η were measured by the drop oscillation method using the following equations:

$$\gamma = \frac{\rho r^3 (2\pi f_2)^2}{8} \quad (1)$$

$$\eta = \frac{\rho r^2}{5\tau} \quad (2)$$

where r is the radius of the melt. f_2 is the mode-2 oscillation frequency, τ is the oscillation decay time. Detailed descriptions of the measurement procedures are provided elsewhere[7,8].

3. Results and Discussion

Figure 1(a) presents the temperature dependence of the density for $(99-x)La_2O_3$–xNb_2O_5–$1Fe_2O_3$ (x = 29, 39, 49, 59, 69, 79, 89, and 99) melts. Most compositions exhibited a linear decrease in density with increasing

temperature. However, the sample with x = 39 displayed a noticeable deviation from linearity around 2000 K, which is close to its liquidus temperature of 1868 K. At a given temperature, the melt density decreased monotonically with increasing x, reflecting the substitution of the heavier La_2O_3 with lighter Nb_2O_5. Downward arrows indicate the glass transition temperature (T_g) of $60La_2O_3$–$40Nb_2O_5$ and $30La_2O_3$–$70Nb_2O_5$ glasses, corresponding to x = 39 and 69, respectively. For both x = 39 and x = 69, density data for the corresponding glasses at room temperature are plotted as triangles. Dashed lines connecting T_g and room temperature exhibit a gentler slope compared to that of the high-temperature melts, which is consistent with the lower thermal expansion coefficients of solids relative to liquids.

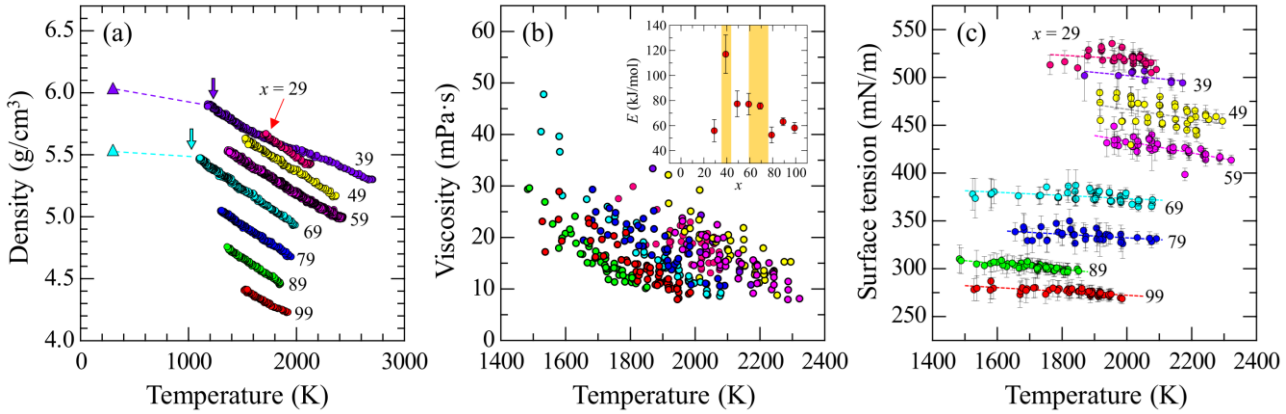

Figure 1 (a) Temperature dependence of the density of (99–x)La_2O_3–xNb_2O_5–1Fe_2O_3 melts. The downward arrows and triangles represent the glass transition temperature and the density of $30La_2O_3$–$70Nb_2O_5$ and $60La_2O_3$–$40Nb_2O_5$ glasses, corresponding to x = 69 and 39, respectively. (b) Temperature dependence of the viscosity. The inset depicts the composition dependence of E. Yellow regions indicate glass-forming regions. (c) Temperature dependence of the surface tension.

Figure 1(b) shows the temperature dependence of melt viscosity. Although limited data points were available for some compositions, viscosity decreased consistently with increasing temperature. The data were analyzed using the Andrade equation:

$$\eta = D\exp\left(\frac{E}{RT}\right) \tag{3}$$

where η is the viscosity, D is the pre-exponential factor, E is the activation energy, R is the gas constant, and T is the temperature. A linear fit of the ln η vs. $1/T$ enabled estimation of E. The inset of Figure 1b displays the composition dependence of E, with yellow regions indicating the glass-forming regions. The sample with x = 39 showed a particularly high E value, while those with x = 49, 59, and 69 also had higher E compared to x = 29, 79, 89, and 99. These trends correlate well with glass-forming regions, where higher E values suggest suppressed ionic mobility and stronger resistance to crystallization. In contrast, lower E values reflect greater ionic mobility, which facilitates crystallization and reduces glass-forming ability.

To further evaluate glass-forming ability, the fragility index m, a key parameter introduced by Angell, was estimated from the temperature dependence of viscosity using the simplified Mauro–Yue–Ellison–Gupta–Allan (MYEGA) model[9]:

$$\log_{10}\eta = -3 + 15\frac{T_g}{T}\exp\left[\left(\frac{m}{15}-1\right)\left(\frac{T_g}{T}-1\right)\right] \tag{4}$$

For melts with x = 39, 59, and 69, the estimated values of m were 86.7, 72.6, and 79.5, respectively. Since a larger m generally indicates a more fragile liquid with lower glass-forming ability, the relatively high m for x = 39 might suggest lower glass-forming ability compared to the others. However, this interpretation contradicts the E values, which suggest strong glass-forming ability for x = 39. This discrepancy may arise from uncertainties in m estimation at high temperatures or from a possible fragile-to-strong transition in this composition range. More accurate viscosity measurements near T_g are required to resolve this issue. For compositions lacking T_g data (x = 29, 49, 79, 89, and 99), m could not be directly estimated, but is presumed to lie in the range of 70–100 assuming similar T_g values to neighboring compositions.

Figure 1(c) presents the temperature dependence of surface tension, which decreased linearly with temperature. Measured values ranged from 250 to 550 mN/m. At 2000 K, the surface tension decreased monotonically with increasing Nb_2O_5 content. The composition dependence at this temperature was fitted by the linear equation: $\gamma_{2000}(x) = (-3.66 \pm 0.23)\cdot x + (627 \pm 21)$. From this fit, the extrapolated surface tensions of pure

La_2O_3 and Nb_2O_5 melts were estimated to be 627 ± 21 and 262 ± 46 mN/m, respectively. These values are in good agreement with previously reported data[10,11], confirming the reliability of the present measurements.

4. Summary

The temperature-dependent density, viscosity, and surface tension of La_2O_3–Nb_2O_5 binary melts were measured using the ISS–ELF. The compositions studied ranged from x = 29 to 99. Density was measured from temperatures above 2300 K down to deeply undercooled states. Viscosity was measured at temperatures above the melting point, within the range of approximately 10^{-1}–10^{-3} Pa·s. The activation energy was determined using the Andrade equation and was found to be dependent on the composition. Higher activation energy values were found in glass-forming regions, indicating reduced ion mobility and an enhanced tendency for glass formation. The fragility index (m) was estimated using the simplified MYEGA equation, revealing that the melts are highly fragile liquids, with m values exceeding 70. Surface tension demonstrated a linear relationship with composition, further supporting the connection between melt properties and glass-forming ability. These results demonstrate that thermophysical parameters obtained under microgravity conditions using ISS–ELF provide valuable indicators for assessing glass-forming ability in unconventional oxide systems.

Acknowledgments

A part of the research was conducted under the FY2016 Kibo feasibility study theme "The origin of fragility in high-temperature oxide liquids - toward fabrication of novel non-equilibrium oxide materials : Fragility" (PI: Shinji Kohara). The authors are grateful to the ISS crew members and the ground operation staff for their support during the onboard experiments. This study was supported in part by JSPS KAKENHI (Grant numbers JP20H02429, JP20H05880, JP20H05882, JP21K18800, and JP25K22156).

Conflicts of Interest

The authors declare no conflict of interest.

References

1) A. Masuno: Functionalities in unconventional oxide glasses prepared using a levitation technique. J. Ceram. Soc. Jpn. **130** (2022) 563, DOI: 10.2109/jcersj2.22073.
2) A. Masuno: Structure of Densely Packed Oxide Glasses Prepared Using a Levitation Technique. J. Phys. Soc. Jpn. **91** (2022) 091003, DOI: 10.7566/JPSJ.91.091003.
3) W. Rhim *et al.*: An electrostatic levitator for high-temperature containerless materials processing in 1-g. Rev. Sci. Instrum. **64**, (1993) 2961, DOI: 10.1063/1.1144475.
4) T. Ishikawa *et al.*: Status of the electrostatic levitation furnace in the ISS – surface tension and viscosity measurements. Int. J. Microgravity Sci. Appl. **39** (2022) 12, DOI: 10.15011/jasma.39.390101.
5) A. Masuno *et al.*: Thermal and optical properties of La_2O_3–Nb_2O_5 high refractive index glasses. Opt. Mater. Express 4 (2014) 710, DOI: 10.1364/OME.4.000710.
6) A. Masuno *et al.*: Drastic connectivity change in high refractive index lanthanum niobate glasses. Chem. Mater. **25** (2013) 3056, DOI: 10.1021/cm401236s.
7) A. Masuno *et al.*: Glass-forming ability of La_2O_3–Nb_2O_5 evaluated via thermophysical properties under microgravity. npj Micogravity, in press, DOI: 10.1038/s41526-025-00520-w.
8) T. Ishikawa *et al.*: Thermophysical property measurements of refractory oxide melts with an electrostatic levitation furnace in the International Space Station. Front. Mater. **9** (2022) 954126, DOI: 10.3389/fmats.2022.954126.
9) Q. Zheng *et al.*: Universality of the high-temperature viscosity limit of silicate liquids. Phys. Rev. B **83** (2011) 212202, DOI: 10.1103/PhysRevB.83.212202.
10) J. Paras *et al.*: The surface tension and density of molten Sc_2O_3, La_2O_3, Y_2O_3, Al_2O_3, and MgO measured via a pendant droplet method. Met. Mater. Trans. B **53** (2022) 2077, DOI: 10.1007/s11663-022-02508-3.
11) N. Ikemiya *et al.*: Surface tensions and densities of molten Al_2O_3, Ti_2O_3, V_2O_5 and Nb_2O_5. ISIJ Int. **33** (1993) 156, DOI: 10.2355/isijinternational.33.156.